Chapter 4

MEASUREMENTS OF CD/CA IN DEEP-SEA CORALS REFLECT VITAL EFFECTS AND SEAWATER CD/CA

Selene F. Eltgroth, Jess F. Adkins, and Diego P. Fernandez

Abstract

We measured Cd/Ca in a suite of modern and fossil deep-sea corals with the goal of extending the use of this nutrient proxy from benthic foraminifera to deep-sea corals. We found modern deep-sea coral Cd/Ca ranging from 0.04 to 1.5 μmol/mol, and six of these corals had anomalously high Cd/Ca with respect to the water in which they grew. Most of these high Cd/Ca corals were also marked by high Cd/Ca variability. We traced the origin of the Cd/Ca variability to a systematic trend in deep-sea corals with increasing Cd/Ca along the upward direction of coral growth. This probable vital effect is especially pronounced in the anomalously high Cd/Ca corals. We conclude that, in the case of these high Cd/Ca corals, the systematic trend in Cd/Ca has effectively obscured the signal of seawater Cd/Ca. When these high Cd/Ca corals are removed from the calibration, a correlation between Cd/Ca_{coral} and Cd/Ca_{water} is observed for the remaining 8 deep-sea corals with a best fit coral-water partition coefficient of 1.3 ± 0.1. We compared two records of Cd/Ca generated from fossil deep-sea corals recovered from the North Atlantic to our modern calibration dataset. We observed that one coral (from 15.4 ka) has low average Cd/Ca and may reflect average environmental Cd/Ca. Because Cd/Ca increases systematically toward the top of this coral, however, the within coral record cannot be

conclusively linked with nutrient composition changes. The other coral (from 12.0 ka) clearly resembles the high Cd/Ca corals of the modern calibration, so its Cd/Ca record is not credible.

Introduction

Phosphate concentrations in the deep North Atlantic serve as a volumetric tracer of deep-water circulation. With a reliable estimate of a conservative or quasi-conservative tracer like phosphate to remove the effect of source water mixing in the Atlantic, an additional radioactive tracer like $\Delta^{14}C$, may be used to determine the ventilation rate of the deep-water. This ventilation rate is essential to understanding the function of the meridional overturning circulation in the regulation of the climate system. With this in mind, our goal is to follow up the deep-sea coral Cd/Ca work of Adkins (1998) to develop this phosphate proxy for use in deep-sea corals.

Relationship Between Cadmium and Phosphate in Seawater

Cadmium profiles in the ocean are similar to profiles of PO_4 (Boyle, Sclater et al. 1976). Although the biological processes governing the seawater Cd distribution remain unidentified, the relationship between Cd and PO_4 below the ocean mixed layer has been described empirically and approximated with a simple box model. The empirical fit to the global data set has two linear portions that meet at a $[PO_4^{3-}]$ of 1.3 μmol/kg (Boyle 1988). This "kink" at 1.3 μmol/kg is thought to be caused by the input of low Cd/PO_4 water from the Subantarctic (40–55S) to intermediate water (Frew and Hunter 1992). The relationship between $[PO_4^{3-}]$ and [Cd] has since been expressed as a curve generated by a two-box

model fit that accounts for the exchange between surface and deep ocean water and the transport of particles containing Cd and PO_4 to the deep ocean where the chemical species are remineralized. The best fit of the model to the data is achieved when Cd is removed to the deep ocean box by particle transport twice as fast as for PO_4 (Elderfield and Rickaby 2000). The result of the model fit is slightly different from the two-line fit. Regardless of the fit that is chosen, the large scatter in the ocean data around the trend (~20%) is such that either fit is adequate to relate $[PO_4^{3-}]_{seawater}$ to $[Cd]_{seawater}$.

Cd/Ca in Foraminiferal Tests

Cd/Ca is an established phosphate proxy in epibenthic foraminiferal tests preserved in ocean sediments (Boyle 1981; Hester and Boyle 1982; Boyle 1988; Boyle 1992) (figure 4.1). The relationship for the partition coefficient ($D_{Cd/Ca}$) that relates Cd/Ca in the foraminiferal carbonate and Cd/Ca in the seawater is:

$$D_{Cd/Ca} = \frac{\left(\frac{Cd}{Ca}\right)_{CaCO_3}}{\left(\frac{Cd}{Ca}\right)_{Water}}. \qquad \text{(equation 4.1)}$$

The coretop calibration for calcitic foraminifera showed that $(D_{Cd/Ca})_{foram}$ described by this equation is dependent on the water depth, with a $D_{Cd/Ca}$ of 1.3 at depths shallower than 1150m that increases linearly to 2.9 at 3000 m and is constant below 3000 m (Boyle 1992). The reason for this depth dependence is not known. Using foraminiferal data from the Ontong Java Plateau in the western equatorial Pacific, McCorkle et al. (1995) found that $D_{Cd/Ca}$ decreases below 3000 m, in disagreement with previous core top results. They demonstrated that $D_{Cd/Ca}$ decreases when the calcite saturation state of the water (ΔCO_3^{2-}) drops below 0–10 μmol/kg. In contrast, the core top calibration for aragonitic foraminifera,

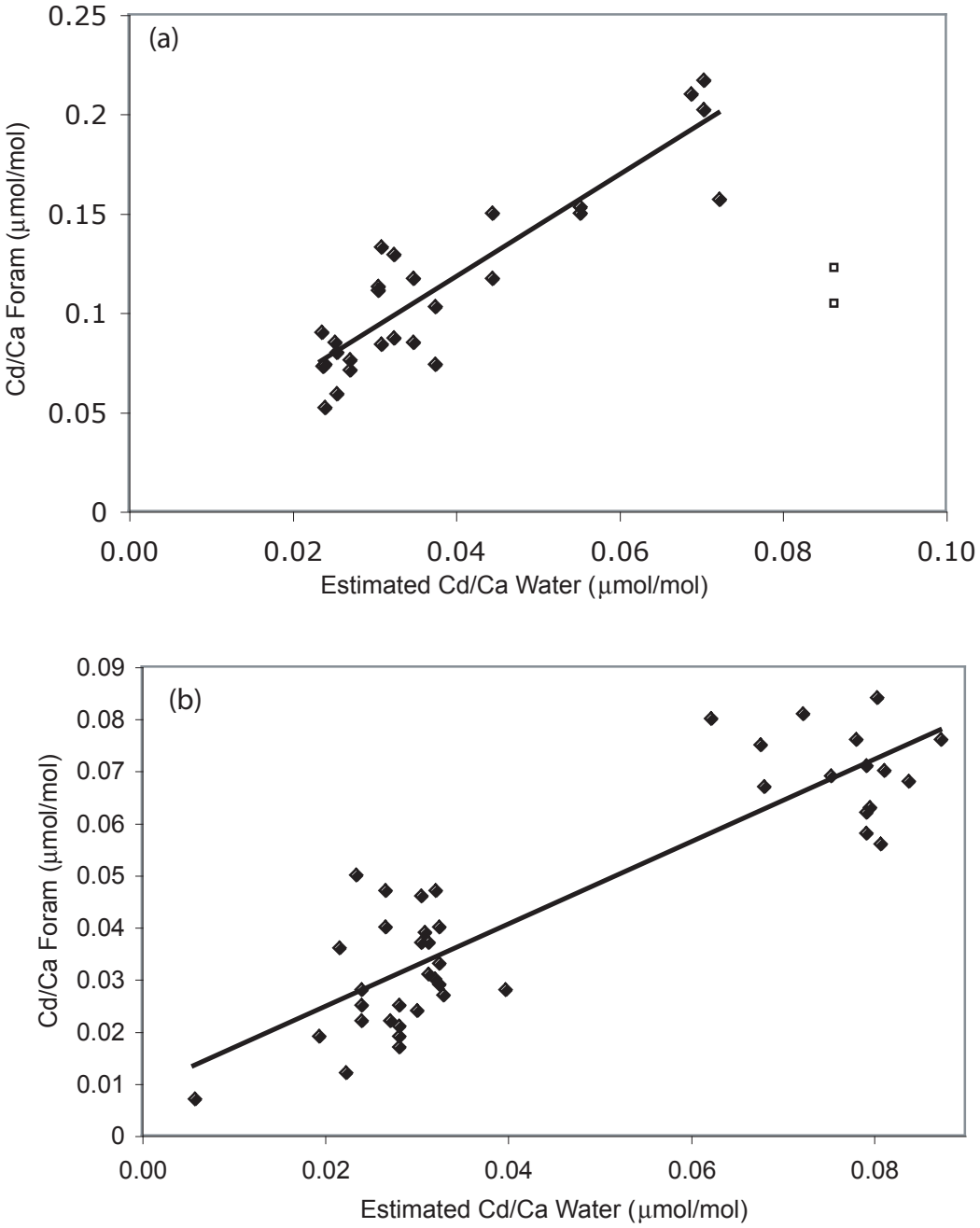

Figure 4.1. Core top Cd/Ca calibrations for (a) calcitic epibenthic forams and (b) aragonitic epibenthic forams. (a) The calcitic foram calibration plot includes foraminifera results from cores deeper than 3000m to avoid variability due to the depth dependence of the Cd/Ca partition coefficient. Each core top also contained at least 15cm of documented Holocene sediment. The data consist of Cd/Ca measurements on the foraminiferal species *Cibicidoides kullenbergi* and *Cibicidoides wuellerstorfi* by Boyle (1988, 1992). The small open squares are questionable data not included in the partition coefficient determination. The best fit partition coefficient through these calcite foraminifera results is 2.56 ± 0.01 (b) The aragonitic foram calibration includes measurements of foraminifieral species *Hoeglundina sp.* by Boyle et al. (1995). The best fit partition coefficient for the aragonitic forams is 0.79 ± 0.02. In both panels, Cd/Ca of the water was estimated from phosphate concentrations from nearby water sampling stations as described in the text.

the same $CaCO_3$ polymorph as stony corals, showed that $D_{Cd/Ca}$ is very near 1.0 with no significant depth dependence (Boyle, Lobeyrie et al. 1995). Corals have three advantages over foraminiferal climate reconstructions because they are not subject to sediment bioturbation, they can be individually dated by U-series techniques, and they are sufficiently massive to accommodate high-resolution records for multiple proxies within the same coral.

Cd/Ca in Surface and Deep-sea Corals

Annually-banded surface coral Cd/Ca has been shown to be a tracer of upwelling in the case of a surface coral from the Galapagos Islands and to track industrial emissions in a coral from Bermuda (Shen, Boyle et al. 1987). These records of surface coral Cd/Ca imply a $D_{Cd/Ca}$ of 1 (Shen, Boyle et al. 1987; Shen and Boyle 1988). Results from a Cariaco Basin coral show a transition in Cd/Ca in 1950 that is interpreted as a change in the upwelling state of the region (Reuer, Boyle et al. 2003). The results from several other surface corals from the Galapagos Islands show a lack of seasonality in Cd/Ca near the western island of Isabela and strong seasonal upwelling near the eastern islands of San Cristobal and Hood (Linn, Delaney et al. 1990; Delaney, Linn et al. 1993). Delaney et al. (1993) note potential uncertainty about reconstructing the concentrations of surface $[PO_4^{3-}]$ from Cd/Ca_{Coral} since different surface coral records from the same location (the Island of Isabela) have disparate Cd/Ca_{Coral} values. The other corals from the eastern Galapagos Islands, however, show unmistakable signals of seasonal upwelling and El Nino/Southern Oscillation events.

Based on the foraminifera and surface coral results, deep-sea corals are a promising new tool for reconstructing past $[PO_4^{3-}]$. A North Atlantic deep-sea coral Cd/Ca record at 15.4 ka showed an increase in Cd/Ca over the coral lifetime that may be interpreted as an

increase in the relative supply of nutrient rich southern source water to the coral growth site (Adkins, Cheng et al. 1998). In this study, we evaluate the accuracy of deep-sea coral Cd/Ca as a true signal of the environment using modern deep-sea corals to calibrate Cd/Ca in deep-sea coral against the Cd/Ca of the ambient seawater. We then compare our calibration result with the deep-sea coral record from 15.4 ka and a new record from the Younger Dryas at 12.0 ka.

Samples and Methods

Our suite of 14 modern *Desmophyllum dianthus* deep-sea corals were collected from the Atlantic, Pacific, and Southern Oceans from depths ranging from 421–2145 m (figure 4.2, table 4.1). We acquired these corals from the Smithsonian collection and other American and French dredge collections. We do not know how or if the samples were chemically treated after collection and prior to our analysis. The corresponding PO_4 concentrations, averaged from the nearest water profile stations compiled in the Joe Reid database, vary from 1.1 to 3.0 μmol/kg.

Deep-water carbonates contain refractory Cd that must be cleaned away before the lattice bound Cd can be precisely measured (Boyle 1981). Our cleaning procedure is designed to clean away non-lattice bound Cd in deep-sea corals, including remnant polyp material in interstitial spaces and secondary Cd precipitates on exposed coral surfaces (typically in the form of black, metal-rich crusts), without re-adsorption of previously liberated Cd from the aragonite lattice during the cleaning process. Our Cd/Ca samples were cut from thecal sections of each coral using a Dremel Tool with a diamond saw

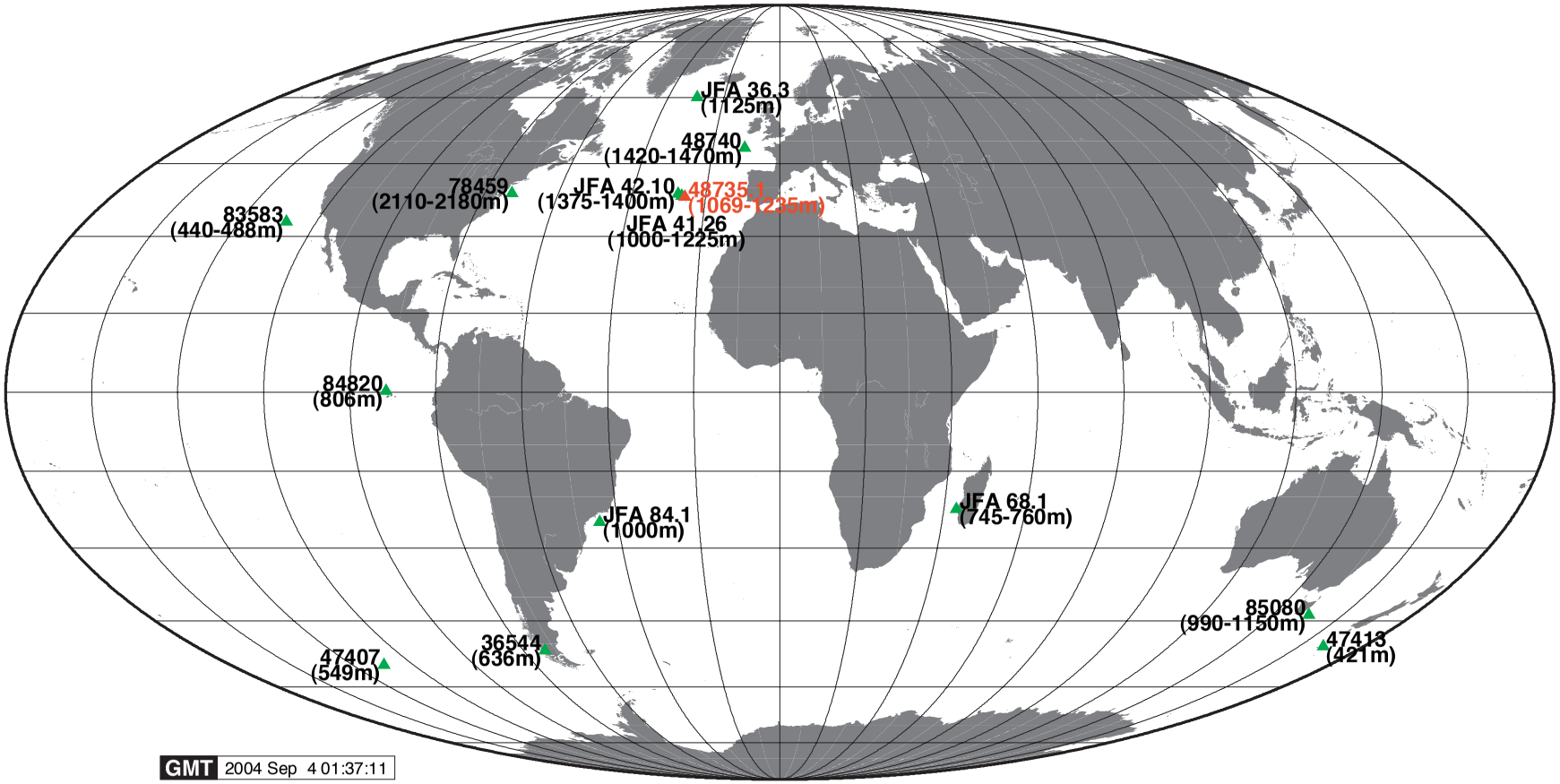

Figure 4.2. Sample map shows the positions and depths of the deep-sea corals analysed in this study.

Coral ID	Depth (m)	Latitude	Longitude	[PO4] (mmol/kg)	Water [Cd] (nmol/kg)	Water Cd/Ca (mmol/mol)
36544	636	51°31'S	73°25'W	1.76	0.455	0.044
47407	549	54°49'S	129°48'W	1.65	0.412	0.040
47413	421	50°38'S	167°38'E	1.61	0.395	0.038
48740	1420-1470	48.4°'N	10.54°'W	1.18	0.248	0.024
78459	2110-2180	38°45'N	72°39'W	1.19	0.249	0.024
83583	488-440	32°54'N	127°47'W	2.92	0.918	0.089
84820	806	0°14'N	91°36'W	2.98	0.943	0.092
85080	990-1150	43°47'S	150°29'E	1.95	0.530	0.051
JFA36.3	1125	60°2.5'N	29°40'W	1.06	0.222	0.022
JFA41.26	1000-1225	38°12.3'N	26°26.1'W	1.08	0.226	0.022
JFA42.10	1375-1400	38°41.4'N	27°33.2'W	1.38	0.301	0.029
JFA68.1	745-760	22°18.9'S	43°1.1'E	1.84	0.485	0.047
JFA84.1	1000	24°54.4'S	44°26'W	2.15	0.610	0.059

Equations:
[PO4]<1.3mmol/kg Cd=.21*[PO4]
[PO4]>1.3mmol/kg Cd=.40*[PO4]-0.25nmol/kg

Table 4.1. Coral Collection Site Data

attachment. The modern corals were observed to be largely free of the dark, metal-rich precipitates that tend to form over time on the exterior surfaces of older deep-sea carbonates, but the outer layer of carbonate was mechanically abraded away as the first step in the cleaning process as a precaution. The rigorous chemical cleaning steps we used were developed to treat foraminifera and have been adapted for use with corals (Boyle 1981; Boyle and Keigwin 1985/86; Shen and Boyle 1988; Boyle 1995; Boyle and Rosenthal 1996). The cleaning method has been described in detail with respect to deep-sea corals by Adkins (1998) and appears in the appendix following this chapter. The key procedures in the chemical cleaning process are ultrasonication to disaggregate fine particles from the coral aragonite, oxidation to oxidize organic matter, reduction to reduce and dissolve metal oxides, and several nitric acid leaches to strip away any metals adsorbed on the aragonite surface (Boyle and Rosenthal 1996). The initially large ivory colored pieces (10–100 mg) were precleaned. The resulting large pieces were crushed and sieved for 250–710 μm size fraction, small enough to allow rigorous cleaning but large enough to reduce the surface area available for Cd adsorption during the cleaning process. Approximately 0.50 mg (1–3 crushed pieces) were measured out for the rigorous trace metal cleaning in 0.5 mL centrifuge tubes. The pieces were chemically cleaned and acid leached then transferred to clean centrifuge tubes. The samples were acid leached one final time before dissolution in 250 μL 2% HNO_3. We also cleaned one surface coral blank (*Porites sp.* acquired from Dr. G. Shen) with each set of ~10 samples to ensure that the coral cleaning process did not add any extra Cd to the samples.

Cd/Ca analytical tools include atomic absorption spectrometry (AAS) (Boyle 1981; Boyle and Keigwin 1985/86; Boyle 1995), thermal ionization mass spectrometry (Rickaby, Greaves et al. 2000) and inductively coupled plasma mass spectrometry (ICP-MS) (Lea and Martin 1996; Rosenthal, Field et al. 1999). Our sample analysis was performed by isotope dilution on a Finnegan ELEMENT ICP-MS equipped with a Scott Type Spray Chamber and ESI Teflon nebulizer. We perform our Cd and Ca analyses separately.

For Cd, ^{110}Cd is our spike isotope, and ^{114}Cd is our natural isotope. Our spike is 93.63 ± 0.07% ^{110}Cd and 1.21 ± 0.02% ^{114}Cd ($^{110}Cd/^{114}Cd_{spike}$ = 77.4 ± 1.3). The spike solution was diluted to a total cadmium concentration of 3.193×10^{-12} mol/g. The natural abundances are 12.49% and 28.73% for ^{110}Cd and ^{114}Cd, respectively ($^{110}Cd/^{114}Cd_{sample}$ = 0.4347). We corrected for the Sn interference at mass 114 by measuring ^{120}Sn and multiplying this measured intensity by the natural abundance ratio (0.65%/32.59%). We mix 100 μL of our dissolved sample solution with 100 μL of our Cd spike solution to create our analytical solutions. We monitor accuracy with a spiked gravimetric standard (SGS) of known isotopic ratio. The measured SGS ratio is corrected back to $^{110}Cd/^{114}Cd$ = 1.605, and this correction factor is applied to each analysis to account for changing instrument fractionation.

We used two separate mass spectrometric methods to measure Ca. We measured Ca alone in our early samples (run ID α–αρ) and later developed a mixed spike for the simultaneous measurement of Mg, Ca, and Sr (run ID ασ–βε). For Ca in our early samples, we measured ^{43}Ca as our spike isotope and ^{48}Ca as our natural isotope. Our original Ca

spike solution had ^{43}Ca of 83.93% and ^{48}Ca of 0.09% ($^{43}Ca/^{48}Ca$ = 933). The total calcium concentration of this original solution was $1.578x10^{-8}$ mol/g. A 50 μL aliquot of the sample primary solution was diluted by adding 500 μL 5% nitric acid. Analytical solutions were made up of 100 μL of this sample secondary solution mixed with 100 μL of the spike solution. For the samples mixed with the multispike, the interference caused by $^{86}Sr^{++}$ at mass 43 is corrected by measuring the intensities at masses 43.5, 86, and 87 and the intensity of the interference is calculated using the doubly to singly ionized ratio for ^{87}Sr and multiplying this ratio by the intensity at ^{86}Sr. The properties of our mixed Mg, Ca, Sr spike are: $^{25}Mg/^{24}Mg$ = 91.01, $^{43}Ca/^{48}Ca$ = 932.6, $^{87}Sr/^{88}Sr$ = 11.03. Spike concentrations are [^{24}Mg] = 0.2447 nmol/g, [^{43}Ca]=0.1503 nmol/g, and [^{88}Sr] = 5.315 nmol/g. The natural abundances of Ca are 0.135% and 0.187% for ^{43}Ca and ^{48}Ca, respectively ($^{43}Ca/^{48}Ca$ = 0.722). Our analytical solutions were made up of 40 μL of the mixed spike, 20 μL of the sample primary, and 1 mL 5% HNO_3.

Our ICP-MS sample sequence order is listed in table 4.2. We increased the frequency with which SGSs were run to account for changes in instrument fractionation over time. For the ICP-MS analysis, we ran 70 passes for each Ca analysis and 75 passes for each Cd analysis. The Ca run is slightly shorter to account for a longer take up time needed for Ca. The analytical blank (5% nitric acid) was used to correct for instrument background. Interspersed with samples are measurements of the SGS to monitor and correct sample ratios for instrument fractionation (figure 4.3). Our SGS results show a high degree of variability for run IDs αψ and αω. The measured intensities show irregular fluctuations that are the reason for the observed variability, but the peak shapes look

Early Samples (α–αμ)	**Later Samples (αν–βε)**
Blank	Blank
SGS	SGS
Blank	Blank
6 Samples	3 Samples
2 CS	3 CS
Blank	
6 Samples	* We repeat this basic
2 CS	structure up to 10
Blank	times until all samples
6 Samples	are measured
2 CS	
Blank	
6 Samples	
2 CS	
Blank	
6 Samples	
2 CS	
Blank	
SGS	

Table 4.2. ICP-MS Sequence Structure

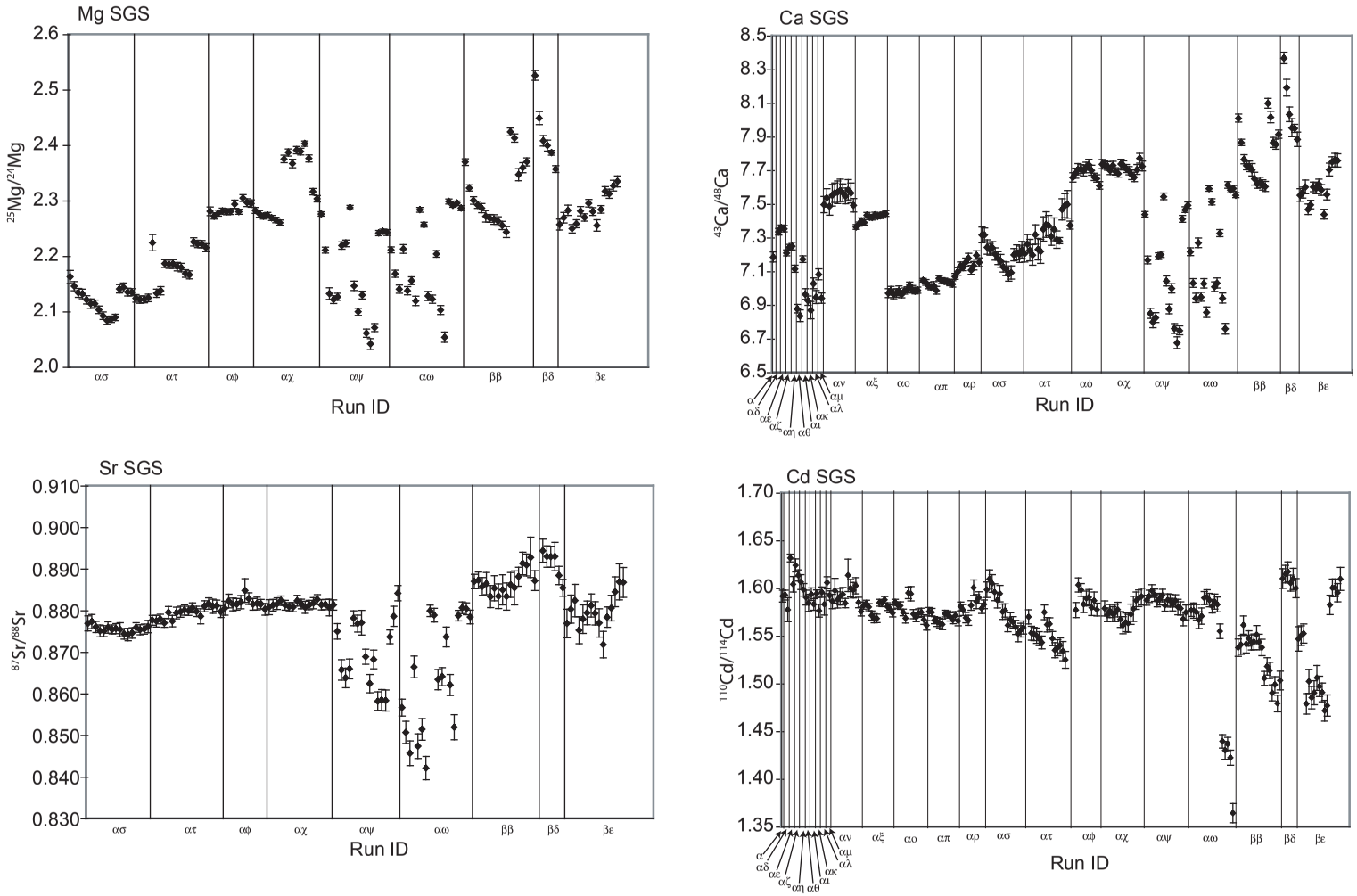

Figure 4.3. Spiked gravimetric standards (SGSs) used to correct our sample ratios for analytical effects are plotted by run ID. Error bars reflect 2σ standard errors based on multiple scans of each sample. Early measurements (α to αμ) used only 2 SGS analyses per run, which were not sufficient to account for instumental drift over the sample analyses. SGS ratio "jumps" are due to changes in the instrumental tuning parameters and recentering of peaks. Large drift in the SGS ratios is generally due to changes in peak position over time. Ca and Cd SGSs were measured over all runs (α to βε). Mg and Sr were added to the analytical method when the Mg, Ca, Sr mixed spike replaced the Ca only spike. Therefore, the Mg and Sr data are limited to runs ασ through βε.

normal. We are unsure of the reason for the instrument unpredictability. To evaluate the precision of our measurements we also repeatedly analyzed two consistency standards (figure 4.4). We observe a shift in the measured [Ca] after run αξ. At that time, we noticed that the Ca spike solution had been evaporating from its storage container. We replaced the container with another and stored the solution in a more humid environment and the [Ca] precision improved. Precision for the consistency standard was 6% (all runs) and 4% for runs αο to βε (2σ standard deviation), after we fixed the Ca spike issue. We verified our ICP-MS results by analyzing our consistency standards by AAS. Furthermore, our deep-sea coral results agree with those of Adkins (1998), who analyzed the same deep-sea samples from the Smithsonian collection using an AAS technique.

Results and Discussion

We studied 14 modern deep-sea corals for Cd/Ca and analyzed 8–39 discrete samples from each (figure 4.5). The Cd/Ca_{water} corresponding to our deep-sea coral sample sites was calculated by applying the Boyle 2-line relation to the PO_4^{3-} seawater data to determine [Cd] and dividing by [Ca]=10.3 mmol/mol. The resulting Cd/Ca_{water} varies from 0.02 to 0.10 μmol/mol (table 4.1). Our Cd/Ca_{coral} results range from 0.04–1.5 μmol/mol, a much larger span than Cd/Ca_{water} (tables 4.3 and 4.4). No clear $D_{Cd/Ca}$ can be determined from all of the data. We observe that six of the samples have elevated Cd/Ca_{coral} (average value 0.2–1.2 μmol/mol) and most of these corals additionally have substantial variability. In contrast, eight samples have significantly smaller Cd/Ca_{coral} (0.04–0.16 μmol/mol) and generally smaller variability. If we focus in on the set of corals with smaller Cd/Ca_{coral}, we estimate that the partition coefficient ($D_{Cd/Ca}$) is 1.3 ± 0.1. We illustrate this in figure 4.5b

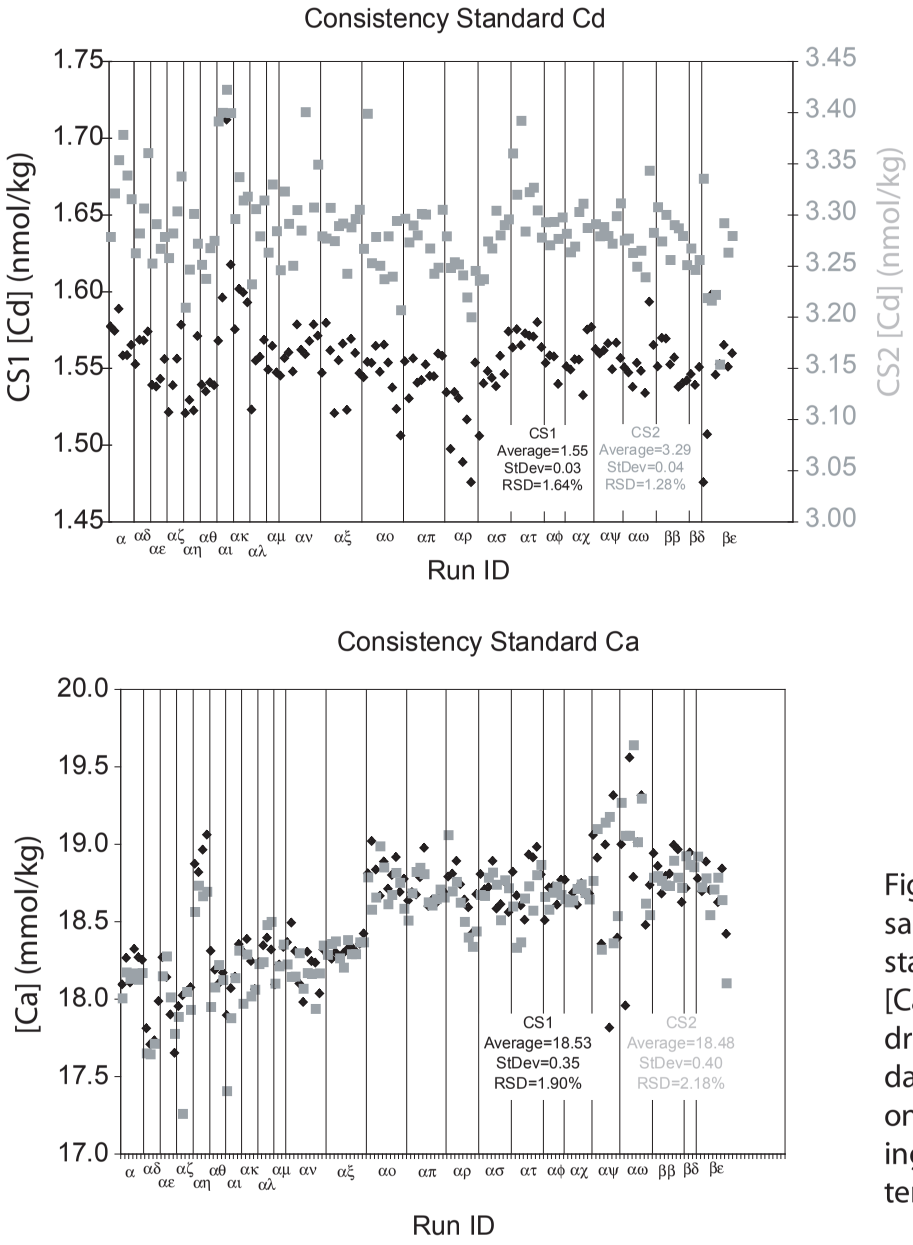

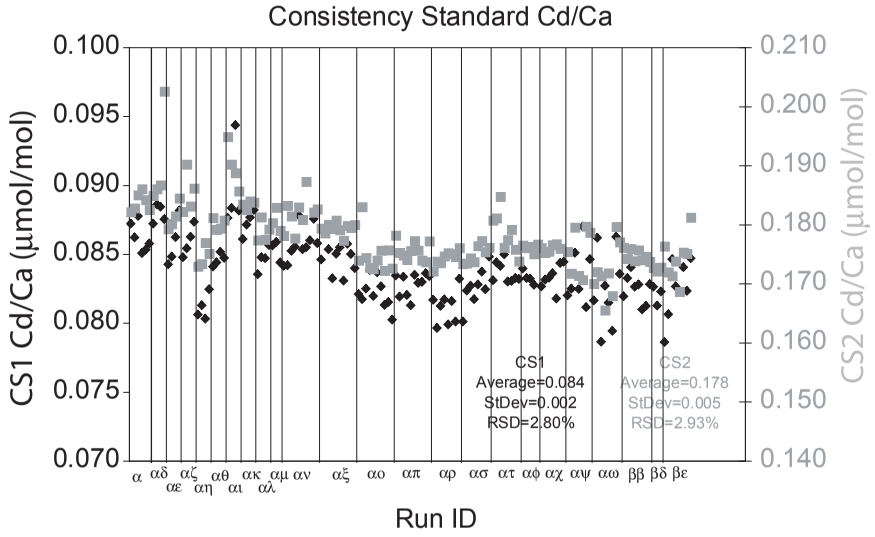

Figure 4.4. Two consistency standards run with each batch of samples give an overall Cd/Ca measurement precision of 6% (2σ standard deviation). Most of the variability is driven by changes in [Ca]. When we consider only standards run αο to βε, the precision drops to 4% (2σ standard deviation). Note that consistency standard [Ca] does not change when the spike is changed from Ca only to the Mg,Ca,Sr mixed spike starting with run ID ασ, indicating that our Ca only and mixed spike concentrations are consistent with one another.

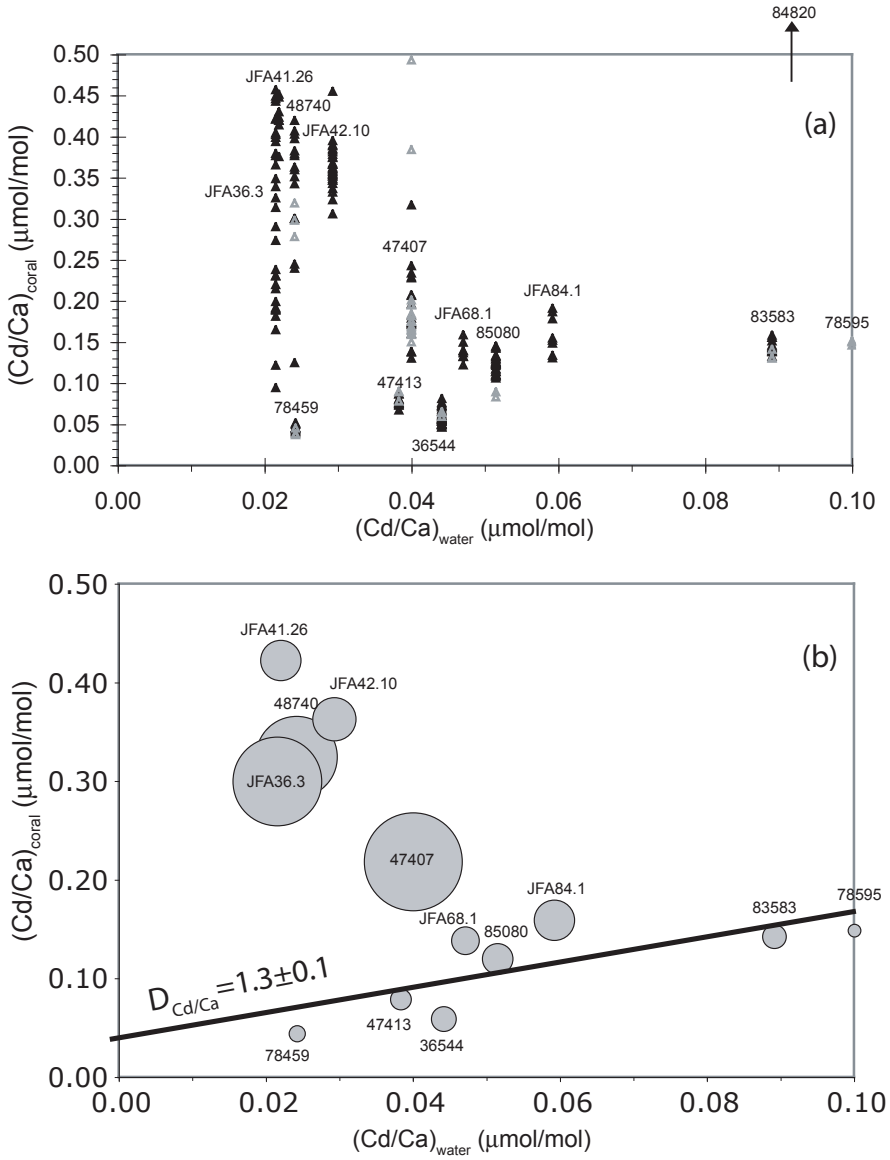

Figure 4.5. Cd/Ca deep-sea coral calibration results. (a) The results from coral 84820 (indicated by the arrow) plot off scale and range from 0.5 to 1.5 µmol/mol). The ICP-MS results from this study are marked by solid black triangles while the AAS results by Adkins (1998) are marked by gray triangles. (b) The same data plotted to emphasize differences in average Cd/Ca and within-coral variation. Each coral is plotted with the size of each data point scaled by the 2σ standard deviation. Based on these results, we divide the corals into 2 groups. High Cd/Ca, high variability corals include JFA36.3, JFA41.26, JFA42.10, 48740, 47407, and 84820. Low Cd/Ca corals with low Cd/Ca variability include 78459, 47413, 36544, JFA68.1, 85080, JFA84.1, 83583, and 78595. We use these low Cd/Ca corals to construct our best guess at the deep-sea coral Cd/Ca partition coefficient. The best fit partition coefficient is $D_{Cd/Ca} = 1.3 \pm 0.1$.

Run ID	Coral ID / Description
α	Consistency standards only
αδ	36544 samples: stepped cleaning >710mm size fraction
αε	36544
αζ	36544
αη	36544
αθ	81408
αι	47407 81408 85080
ακ	36544 stepped cleaning
αλ	47413 48740 83583
αμ	81408 84820
αν	78459 JFA42.10 JFA68.1
αξ	JFA41.26 JFA36.3 JFA84.1
αο	47413 stepped cleaning
απ	JFA42.10 stepped cleaning
αρ	85080 JFA41.26 36544 47407 JFA36.3 JFA84.1
ασ	47407 48740 85080 83583 47413 36544 78459 84820
ατ	78459 47413 85080 36544 47407 84820 83583 48740 47407
αφ	85080 horizontal cross-section
αχ	JFA42.10 horizontal cross-section
αψ	JFA36.3 vertical thecal section
αω	36544 vertical thecal section
ββ	JFA36.3 vertical septal section
βδ	36544 10-40μm standard
βε	48735.1 (Younger Dryas) vertical thecal section

Table 4.3. ICP-MS Run Description

Coral ID	Run ID	$(Mg/Ca)_{coral}$ (mmol/mol)	$(Sr/Ca)_{coral}$ (mmol/mol)	$(Cd/Ca)_{coral}$ (μmol/mol)	Average $(Cd/Ca)_{coral}$ (μmol/mol)	2σ
47407	αι	-	-	0.234	0.192	0.070
		-	-	0.160		
		-	-	0.172		
		-	-	0.173		
		-	-	0.171		
		-	-	0.138		
		-	-	0.243		
		-	-	0.228		
		-	-	0.206		
85080	αι	-	-	0.126	0.123	0.021
		-	-	0.132		
		-	-	0.142		
		-	-	0.134		
		-	-	0.130		
		-	-	0.132		
		-	-	0.121		
		-	-	0.129		
		-	-	0.144		
		-	-	0.145		
	ασ	1.12	9.00	0.125		
		1.28	10.28	0.125		
	ατ	1.35	10.19	0.108		
		1.16	10.19	0.124		
		1.45	10.41	0.123		
	αϕ	1.77	9.98	0.114		
		1.71	10.50	0.110		
		1.48	10.20	0.117		
		0.96	10.19	0.124		
		1.34	10.30	0.124		
		1.60	10.59	0.106		
		1.29	10.20	0.117		
		1.56	10.57	0.109		
		1.70	10.32	0.109		
		1.28	10.20	0.123		
		1.82	9.97	0.110		
		1.46	10.01	0.114		
		1.36	10.17	0.123		
		1.62	10.17	0.114		

Table 4.4. *D. dianthus* Trace Metal Results

Coral ID	Run ID	$(Mg/Ca)_{coral}$ (mmol/mol)	$(Sr/Ca)_{coral}$ (mmol/mol)	$(Cd/Ca)_{coral}$ (μmol/mol)	Average $(Cd/Ca)_{coral}$ (μmol/mol)	2σ
36544	ακ	-	-	0.053	0.059	0.018
		-	-	0.058		
		-	-	0.061		
		-	-	0.055		
		-	-	0.057		
		-	-	0.054		
		-	-	0.054		
	ασ	1.42	9.93	0.056		
		1.21	9.80	0.050		
		1.29	10.12	0.055		
	ατ	1.29	10.01	0.050		
		1.51	10.05	0.057		
		1.34	10.12	0.056		
	αω	1.45	9.98	0.051		
		1.64	10.02	0.046		
		1.27	9.82	0.049		
		0.79	10.21	0.073		
		0.80	10.27	0.060		
		1.07	10.20	0.068		
		0.88	10.18	0.065		
		1.21	9.46	0.072		
		1.30	9.77	0.049		
		1.56	9.89	0.049		
		1.12	10.30	0.056		
		0.94	10.02	0.056		
		0.79	10.26	0.071		
		0.79	10.29	0.073		
		0.83	10.11	0.075		
		0.77	10.10	0.076		
		1.61	9.81	0.047		
		1.03	10.05	0.053		
		1.52	9.95	0.049		
		1.04	10.08	0.066		
		0.70	10.43	0.058		
		0.87	10.17	0.062		
		1.01	9.99	0.081		

Table 4.4. *D. dianthus* Trace Metal Results (continued)

Coral ID	Run ID	$(Mg/Ca)_{coral}$ (mmol/mol)	$(Sr/Ca)_{coral}$ (mmol/mol)	$(Cd/Ca)_{coral}$ (μmol/mol)	Average $(Cd/Ca)_{coral}$ (μmol/mol)	2σ
47413	αλ	-	-	0.075	0.077	0.011
		-	-	0.079		
		-	-	0.073		
		-	-	0.075		
		-	-	0.087		
		-	-	0.087		
	ασ	1.73	10.20	0.081		
		1.58	10.07	0.076		
		1.63	10.28	0.077		
	ατ	1.63	10.21	0.080		
		1.51	10.04	0.067		
		1.70	10.03	0.074		
83583	αλ	-	-	0.155	0.145	0.015
		-	-	0.146		
		-	-	0.143		
		-	-	0.151		
		-	-	0.139		
		-	-	0.145		
		-	-	0.158		
		-	-	0.142		
	ασ	1.16	10.20	0.155		
		0.88	10.32	0.138		
		0.85	10.26	0.138		
	ατ	0.88	10.37	0.140		
		0.86	10.12	0.132		
		0.98	10.30	0.143		
48740	αλ	-	-	0.420	0.325	0.176
		-	-	0.406		
		-	-	0.379		
		-	-	0.383		
		-	-	0.360		
		-	-	0.397		
		-	-	0.351		
		-	-	0.377		
	ασ	0.95	8.87	0.245		
		1.03	10.27	0.300		
		1.10	10.30	0.363		
		1.09	8.99	0.342		
		1.15	10.08	0.300		
		0.98	10.22	0.240		
	ατ	1.15	10.66	0.403		
		1.21	10.24	0.125		
		1.30	10.21	0.132		

Table 4.4. *D. dianthus* Trace Metal Results (continued)

Coral ID	Run ID	$(Mg/Ca)_{coral}$ (mmol/mol)	$(Sr/Ca)_{coral}$ (mmol/mol)	$(Cd/Ca)_{coral}$ (μmol/mol)	Average $(Cd/Ca)_{coral}$ (μmol/mol)	2σ
84820	αμ	-	-	1.323	1.258	0.385
		-	-	1.525		
		-	-	1.419		
		-	-	0.941		
		-	-	1.106		
		-	-	0.869		
		-	-	1.461		
	ασ	1.21	10.35	1.315		
		0.90	10.67	1.154		
		1.24	10.52	1.179		
	ατ	1.37	10.62	1.442		
		1.31	10.49	1.363		
		1.29	10.52	1.253		
JFA68.1	αν	-	-	0.159	0.139	0.021
		-	-	0.149		
		-	-	0.137		
		-	-	0.132		
		-	-	0.122		
		-	-	0.139		
		-	-	0.140		
		-	-	0.133		
JFA84.1	αξ	-	-	0.152	0.159	0.043
		-	-	0.155		
		-	-	0.134		
		-	-	0.148		
		-	-	0.187		
		-	-	0.178		
		-	-	0.191		
		-	-	0.130		
JFA41.26	αξ	-	-	0.375	0.423	0.044
		-	-	0.448		
		-	-	0.430		
		-	-	0.451		
		-	-	0.414		
		-	-	0.419		
		-	-	0.420		
		-	-	0.423		

Table 4.4. *D. dianthus* Trace Metal Results (continued)

Coral ID	Run ID	$(Mg/Ca)_{coral}$ (mmol/mol)	$(Sr/Ca)_{coral}$ (mmol/mol)	$(Cd/Ca)_{coral}$ (μmol/mol)	Average $(Cd/Ca)_{coral}$ (μmol/mol)	2σ
JFA42.10	αν	-	-	0.363	0.363	0.052
		-	-	0.352		
		-	-	0.352		
		-	-	0.337		
		-	-	0.332		
		-	-	0.347		
		-	-	0.374		
		-	-	0.375		
	αχ	1.03	10.08	0.366		
		1.06	10.60	0.360		
		1.18	10.17	0.384		
		1.30	9.78	0.356		
		1.34	10.10	0.385		
		1.11	10.22	0.395		
		1.39	10.10	0.368		
		0.97	9.99	0.354		
		1.26	9.75	0.306		
		1.50	10.06	0.358		
		1.27	9.95	0.366		
		1.38	10.06	0.346		
		1.14	10.06	0.349		
		1.15	9.99	0.361		
		1.18	10.01	0.343		
		0.75	10.15	0.389		
		0.85	10.00	0.378		
		1.32	10.44	0.455		
		0.71	11.19	0.358		
		0.84	9.82	0.390		
		1.35	9.89	0.381		
		1.23	9.92	0.323		
		0.77	10.34	0.355		
78459	αν	-	-	0.044	0.045	0.007
		-	-	0.041		
		-	-	0.045		
		-	-	0.044		
		-	-	0.051		
		-	-	0.045		
		-	-	0.046		
	ασ	1.18	10.19	0.044		
		1.06	10.12	0.042		
		1.13	10.18	0.049		
	ατ	1.24	10.31	0.051		
		1.14	10.32	0.046		
		1.26	10.12	0.039		

Table 4.4. *D. dianthus* Trace Metal Results (continued)

Coral ID	Run ID	$(Mg/Ca)_{coral}$ (mmol/mol)	$(Sr/Ca)_{coral}$ (mmol/mol)	$(Cd/Ca)_{coral}$ (μmol/mol)	Average $(Cd/Ca)_{coral}$ (μmol/mol)	2σ
JFA36.3	αξ	-	-	0.404	0.300	0.212
		-	-	0.325		
		-	-	0.446		
		-	-	0.399		
		-	-	0.394		
		-	-	0.348		
		-	-	0.449		
		-	-	0.402		
	αψ	1.29	10.39	0.094		
		1.39	10.70	0.214		
		1.40	10.66	0.273		
		1.44	10.57	0.165		
		1.34	11.09	0.230		
		1.02	9.87	0.290		
		0.95	10.23	0.421		
		1.22	10.50	0.421		
		1.38	10.53	0.379		
		1.46	10.55	0.220		
		1.43	10.63	0.199		
		1.46	10.51	0.121		
		1.32	10.81	0.190		
		1.33	10.17	0.189		
		1.35	10.73	0.339		
		1.25	10.50	0.443		
		1.28	10.61	0.377		
		1.39	10.84	0.238		
		1.40	10.29	0.190		
		1.44	10.73	0.192		
		1.30	10.96	0.181		
		1.28	10.31	0.230		
		1.25	10.83	0.313		
		1.10	10.30	0.365		
		1.31	10.39	0.457		

Table 4.4. *D. dianthus* Trace Metal Results (continued)

where the size of each data point is scaled by the 2σ replicate error. Discarding data without an independent rationale is unreasonable, and we seek to understand the origin of elevated Cd/Ca in deep-sea corals.

To evaluate the source of the elevated Cd/Ca_{coral}, we consider three possible controls on Cd incorporation the coral aragonite sample. (1) Chemical processing in the laboratory could cause an elevation in Cd/Ca_{coral} by introducing a new source of Cd to the sample via cleaning solutions, by concentrating existing Cd in the coral, or by failing to remove extraneous Cd. (2) Coral vital effects could modulate Cd incorporation via biological control over the skeletal precipitation process. (3) Environmental factors at the coral growth site could influence Cd/Ca_{water} or Cd/Ca_{coral}. We shall consider each process in turn.

Our deep-sea coral cleaning procedure was designed purposely to avoid sample contamination with Cd. Each cleaning solution was tested for the presence of Cd and Sn prior to sample analysis. The 30% hydrogen peroxide solution that we initially intended to use contained Sn as a stabilizer and this solution was replaced with unstabilized 30% hydrogen peroxide that was stored in a cold, dark refrigerator to maintain effectiveness. The cleaning solutions used to treat the samples were found to contain no detectable Cd or Sn, ruling out the cleaning treatments steps as a source of new Cd. The results from the surface coral blanks reinforce this observation. The surface coral blanks contained only trace amounts of Cd after the cleaning process, indicating that significant Cd was not gained or concentrated via the cleaning process (figure 4.6).

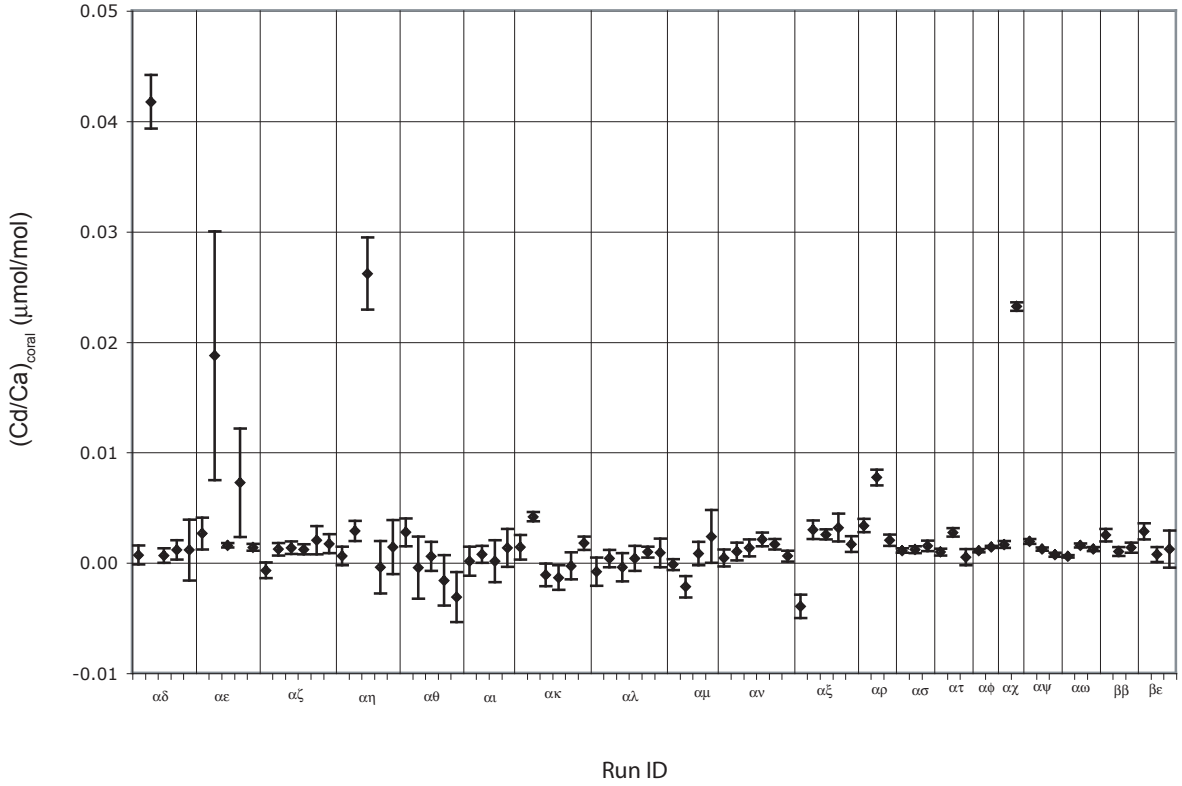

Figure 4.6. Surface coral blank results. We observe the occasional high Cd/Ca, but not of a sufficient magnitude to cause the high Cd/Ca found in the anamalously high Cd/Ca deep-sea corals. Average Cd/Ca in this surface coral is 0.00 ± 0.01 (2σ standard deviation).

We also performed a stepped cleaning test on 3 modern samples, measuring Cd/Ca after each step of the rigorous cleaning procedure and found no increase in Cd/Ca as a result of any cleaning step, indicating that existing Cd was not adsorbed to the aragonite surface and that Ca was not dissolved preferentially to Cd during the leaching steps (figure 4.7). The stepped cleaning did show that the uncleaned samples gave the most precise results, suggesting that the cleaning process may be introducing variability to the samples. Interestingly, the stepped cleaning results also show no decrease in Cd/Ca as the cleaning progresses. Unfortunately, this lack of cleaning progression means that we cannot determine whether the cleaning procedure is effective at removing non-lattice bound Cd. The nonporous structure could possibly isolate the non-lattice bound Cd in the interior of the pieces from the coral cleaning solutions (Shen and Boyle 1988). We believe this result occurs because the non-lattice bound Cd is concentrated in the outer crust of the coral that, in these pristine modern corals, was cleaned away by the mechanical abrasion of the outer surface and precleaning process before the rigorous cleaning. This results applies only to modern sample since fossil samples may have acquired additional Cd contamination over time on the sea floor.

Vital effects in *D. dianthus* have been observed for the stable isotopes $\delta^{13}C$ and $\delta^{18}O$ and the isotopic signal strongly correlates with the coral banding pattern (Adkins, Boyle et al. 2003). Likewise, Mg is concentrated in the optically dense bands in the coral, while Sr is relatively constant throughout a coral (Adkins, Robinson and Fernandez, unpublished data). We first examined Cd/Ca in relation to the coral banding (figure 4.8) and found that Cd/Ca_{coral} does not correlate with coral banding and furthermore, does not

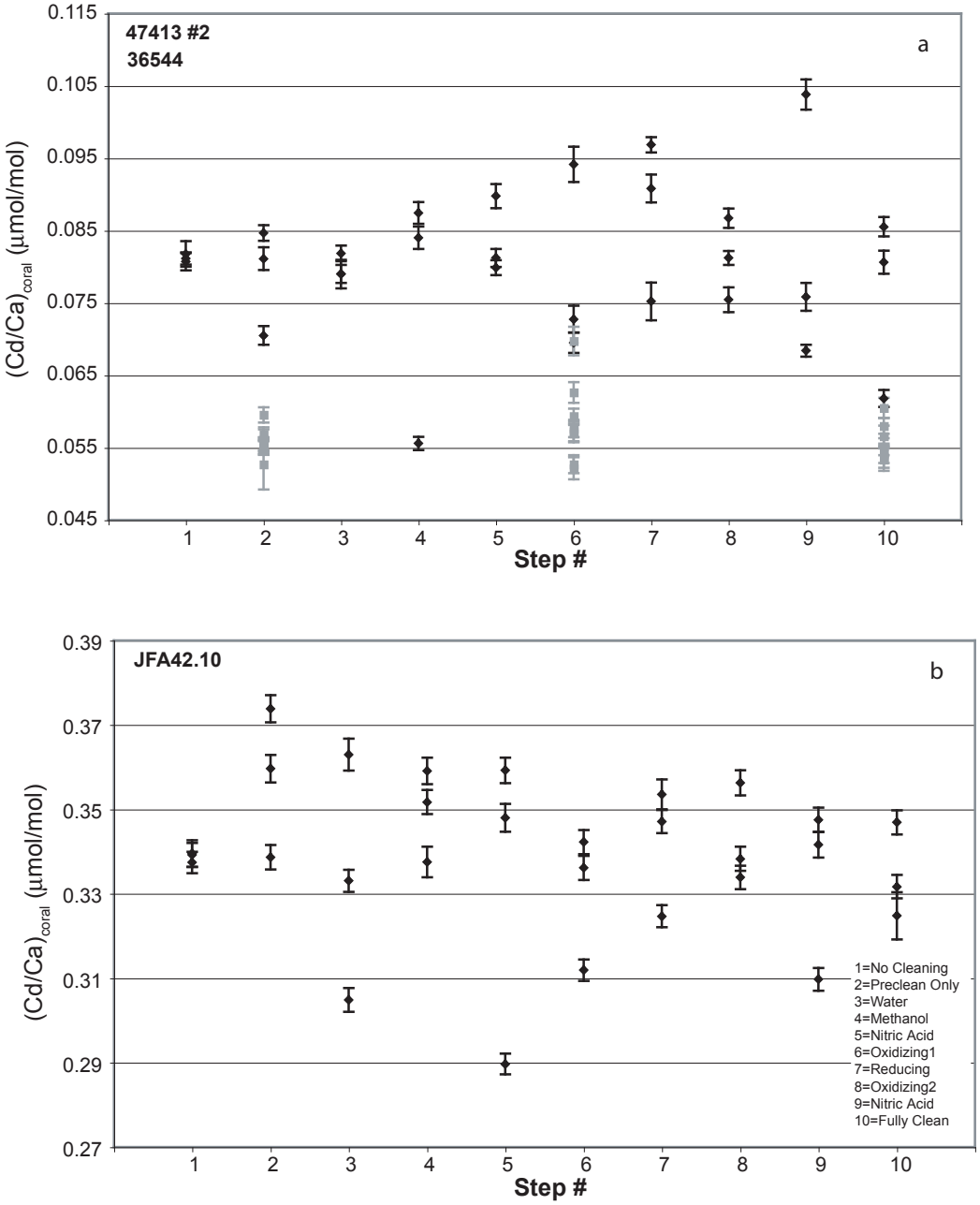

Figure 4.7. Stepped cleaning results from modern *D. dianthus*. (a) The results for low Cd/Ca corals 47413 (run αο) plotted in black and 36544 (run ακ) plotted in gray. (b) The result from high Cd/Ca coral JFA42.10. The step # (x-axis) refers to the cleaning step listed in the lower right. A detailed description of these steps is contained in the appendix at the end of the chapter. The error bars represent the 2σ analytical error on each measurement. None of these corals show reduced Cd/Ca over the cleaning steps. This is probably because the extraneous Cd was removed with the outer crust of these samples before these samples were subject to this part of the cleaning process. Another possibility is that the cleaning steps are unable to access non-lattice bound Cd within each deep-sea coral piece. The data also suggest that the cleaning process may increase the Cd/Ca variability of the samples.

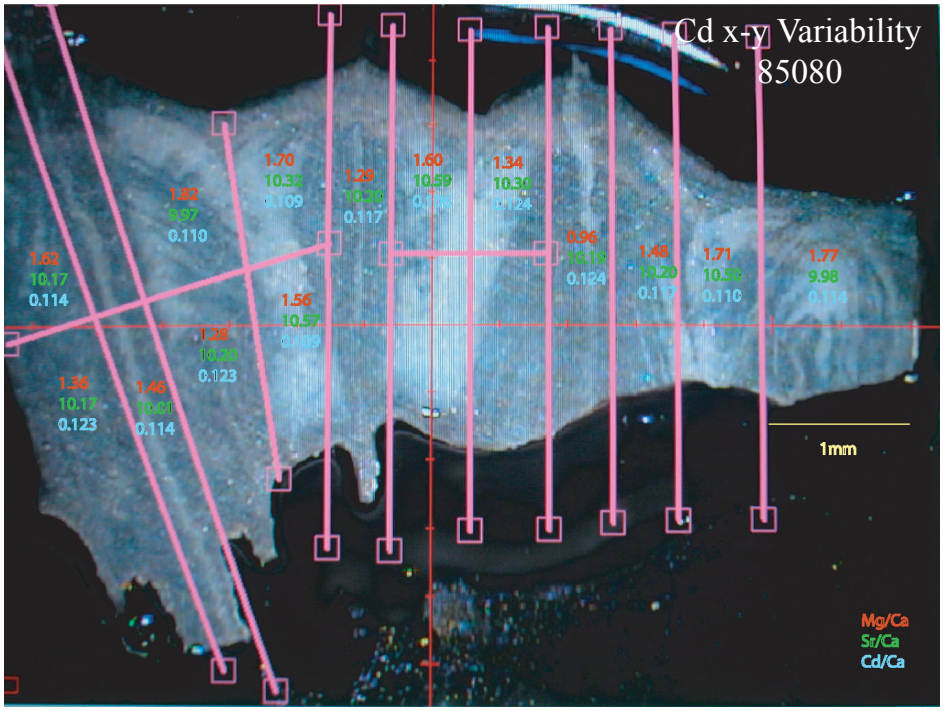

(a)

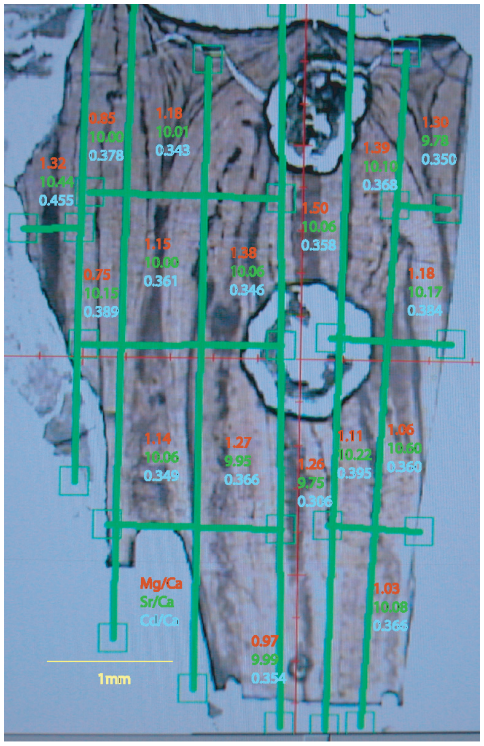

Cd x-y Variability
JFA42.10

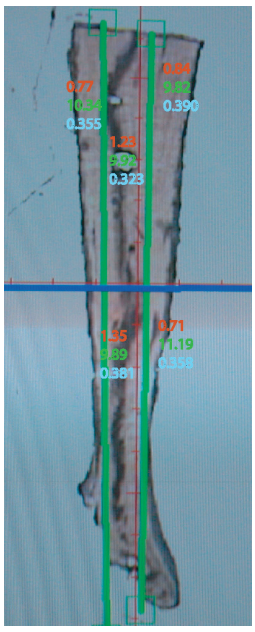

(b)

Figure 4.8. Distribution of Mg/Ca, Sr/Ca, and Cd/Ca in horizontal cross section of *D. dianthus*. (a) Low Cd/Ca coral 85080 under reflected light and (b) high Cd/Ca coral JFA42.10 in transmitted light. These 200mm thick horizontal cross sections were cut along the lines drawn in each image and the resulting pieces cleaned and analyzed for Mg, Ca, Sr, and Cd. Within each section, 3 numbers are listed. These numbers are the Mg/Ca ratio (top/mmol/mol), the Sr/Ca ratio (middle /mmol/mol) and the Cd/Ca ratio (bottom /µmol/mol). Cd/Ca shows no significant correlation with the banding structure of these corals.

correlate with either Mg or Sr (figure 4.9). We then measured Cd/Ca along the trunk of two of the modern deep-sea corals, one from the set of high Cd/Ca corals and the other from the set of low Cd/Ca corals, and we found that Cd/Ca increased to a maximum value toward the top of each coral (table 4.5, figure 4.10). Based on the results from these two corals, we conclude that Cd may be distributed systematically in all *D. dianthus*, with Cd/Ca increasing toward the top of the coral. This trend is especially pronounced in the high Cd/Ca corals and is the origin of the large variability noted in most of these corals. If the cause of the elevated Cd/Ca were attributed to the incomplete cleaning of coral aragonite, this would require a systematic distribution in the non-lattice bound Cd, with more Cd toward the top of the coral. We believe that the likely explanation for the observed trend, however, is that $D_{Cd/Ca}$ in the coral aragonite increased over the lifetime of the coral. In corals with high Cd/Ca, this vital effect is substantial enough to completely overprint the environmental signature.

Investigating the influence of the coral growth process on skeletal Cd/Ca_{coral} is the next step in the development of Cd/Ca_{coral} as a seawater nutrient proxy. With an independent classification scheme, deep-sea coral suitability for Cd/Ca_{water} reconstruction could be determined. A correlation between high-resolution measurements of the coral growth rate and Cd/Ca_{coral} would implicate the process of coral growth as the origin of the observed structure in the Cd/Ca_{coral} record. A Cd/Ca correlation with measurements of chemically similar Zn/Ca would also corroborate coral control over the coral Cd and Zn composition. Duplicating our Cd/Ca results in multiple modern deep-sea corals that grew in the same environment would also be helpful.

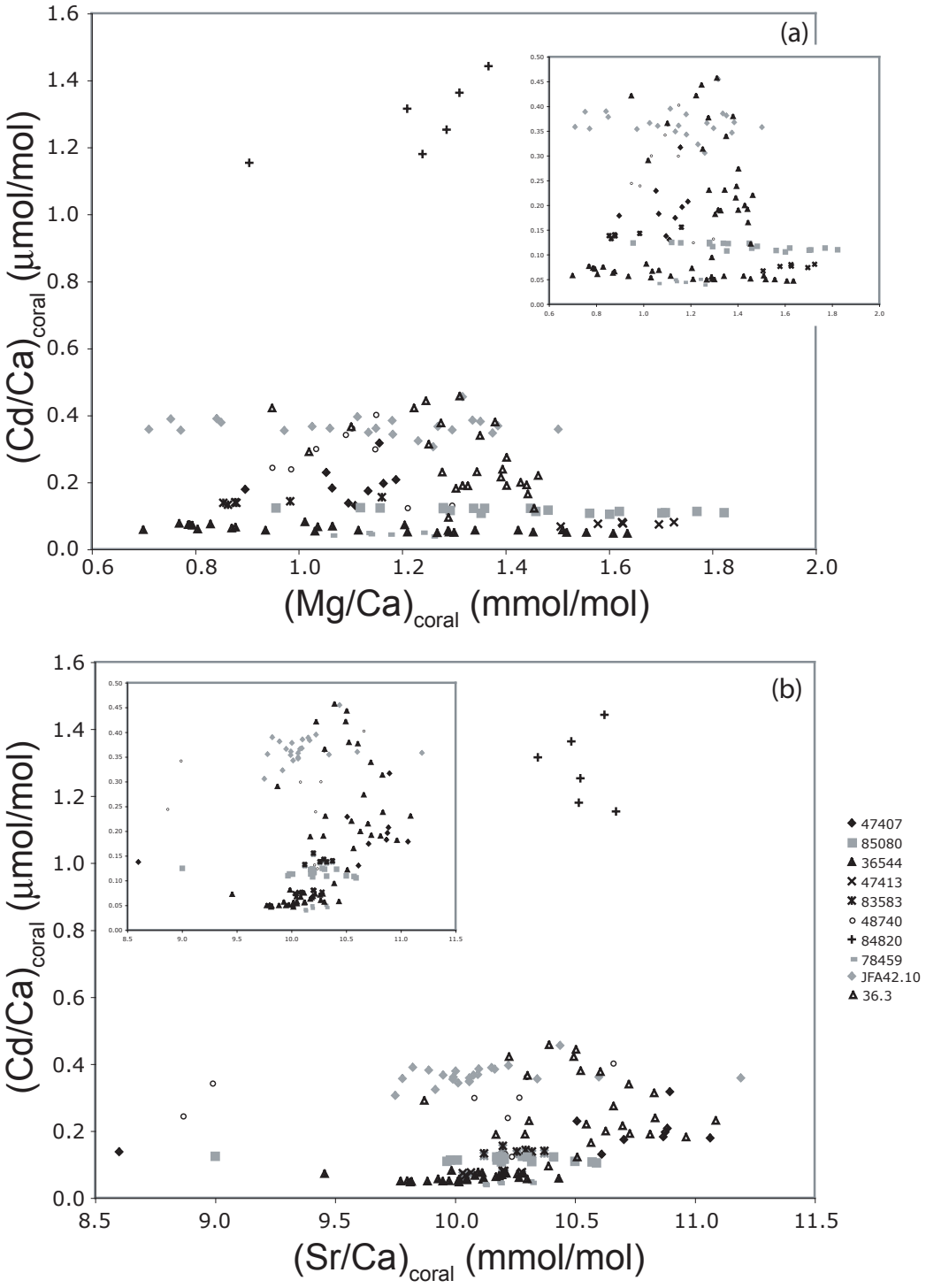

Figure 4.9. Tracer relationships. (a) Most of the corals show no association between Cd/Ca and Mg/Ca. However, the data from high Cd/Ca corals 84820 (+) and 48740 (o) suggest a positive correlation between these tracers. (b) Relationship between Cd/Ca and Sr/Ca shows no correlation between the tracers. In each figure, the nested chart is a zoomed in view of the data. The symbol legend for all plots is shown in the lower right.

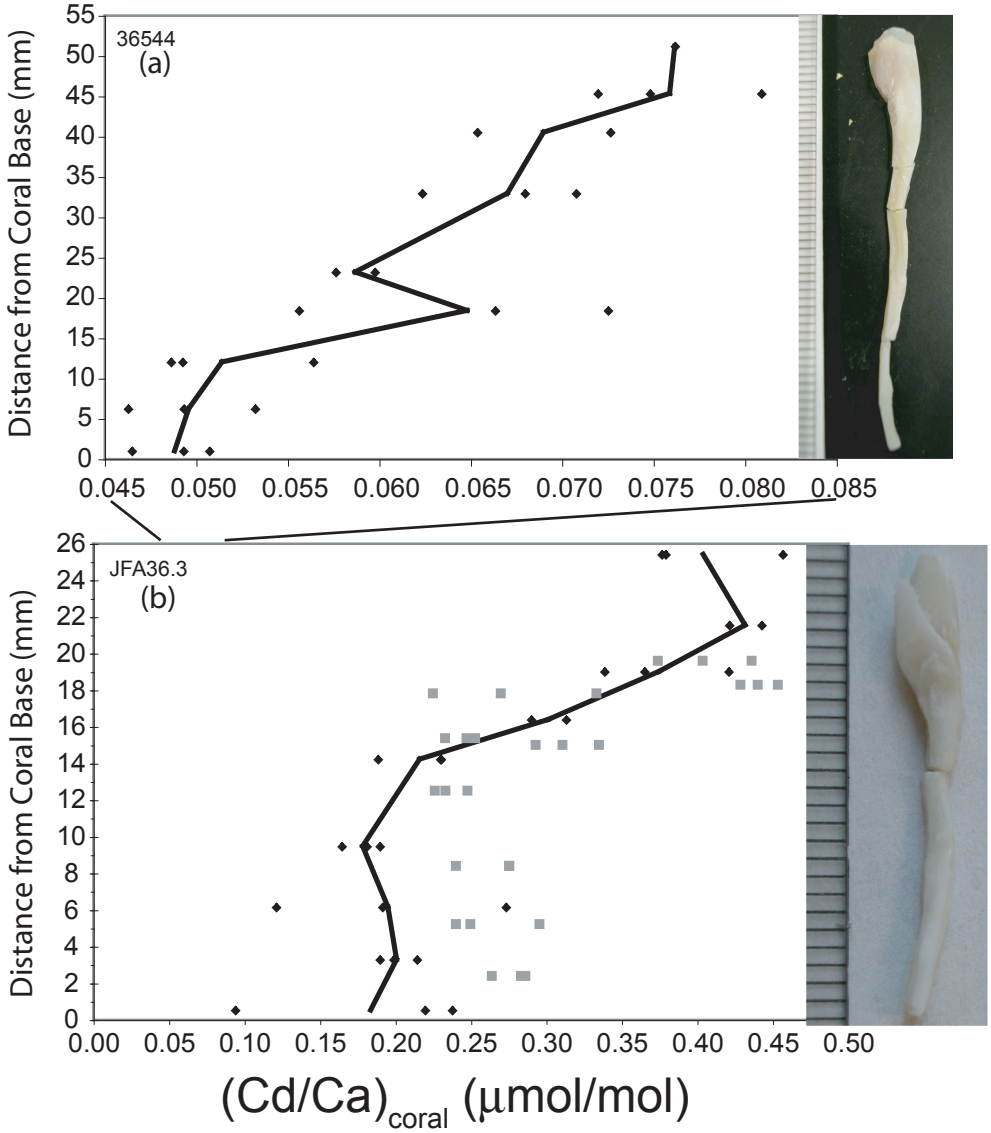

Figure 4.10. Vertical Transects of Cd/Ca in modern deep-sea corals. (a) The top figure is the vertical Cd/Ca record in low Cd/Ca coral 36544. Although the absolute variability is low, there is a trend toward increasing Cd/Ca at the top of the coral. (b) The lower panel shows the record in high Cd/Ca coral JFA36.3. Black diamonds are thecal measurements and gray squares are septal measurements of Cd/Ca in the deep-sea coral.

Coral ID	Run ID	Distance from Coral Base (mm)	$(Cd/Ca)_{coral}$
36544	αω	0.0 - 1.9	0.051
			0.049
			0.047
		5.3 - 7.1	0.046
			0.049
			0.053
		10.5 - 13.5	0.049
			0.056
			0.049
		17.6 - 19.2	0.073
			0.056
			0.066
		21.5 - 24.7	0.060
			0.058
		31.9 - 33.9	0.068
			0.071
			0.062
		39.7 - 41.3	0.065
			0.073
		44.6 - 46.0	0.072
			0.075
			0.081
		50.4 - 52.0	0.076
JFA36.3 thecal	αψ	0 - 1	0.094
			0.220
			0.238
		2.64 - 3.9	0.214
			0.199
			0.190
		5.53 - 6.74	0.273
			0.121
			0.192
		8.32 - 10.58	0.165
			0.190
			0.181
		13.55 - 14.85	0.230
			0.189
			0.230
		15.63 - 17.1	0.290
			0.313
		18.43 - 19.56	0.421
			0.339
			0.365
		20.86 - 22.2	0.421
			0.443
		24.6 - 26.17	0.379
			0.377
			0.457

Table 4.5. Vertical Transect Results

Coral ID	Run ID	Distance from Coral Base (mm)	$(Cd/Ca)_{coral}$
JFA36.3 septal	ββ	1.9 - 2.97	0.283
			0.286
			0.263
		4.51 - 6.02	0.295
			0.240
			0.249
		7.19 - 9.68	0.240
			0.275
			0.275
		11.53 - 13.55	0.233
			0.247
			0.226
		14.75 - 16.09	0.253
			0.247
			0.233
		16.09 - 14.00	0.310
			0.293
			0.334
		16.45 - 19.26	0.366
			0.269
			0.333
		18.43 - 20.86	0.403
			0.374
			0.436
		17.1 - 19.56	0.453
			0.440
			0.428
48735.1	βε	3.49 - 5.53	0.243
			0.157
			0.371
		9.83 - 11.13	0.216
			0.287
			0.394
		15.64 - 17.34	0.400
			0.357
			0.532
		21.58 - 23.29	0.472
			0.584
			0.497
		28.23 - 29.53	0.547
			0.101
			0.519
		30.6 - 31.34	0.657
			0.602
			0.608
		33.72 - 36.26	0.671
			0.689
			0.693
		37.31 - 39.53	0.602
			0.627
			0.705
		39.53 - 41.83	0.586
			0.670
			0.630

Table 4.5. Vertical Transect Results (continued)

Another distinguishing feature linking 5 of the 6 high Cd/Ca deep-sea corals is their geographical origin. Five of the high Cd/Ca corals were collected from the eastern North Atlantic and they plot as a cluster in the upper left of figure 4.5. The coral with the highest Cd/Ca_{coral} was collected near the Galapagos Islands, however, so the high Cd/Ca corals cannot be ascribed to one particular geographical region. The Cd/Ca range in the corals from the North Atlantic is very large, even though the corals grew within the last few hundred years when the Cd/Ca of the deep-water was very stable. The most proximate cause of Cd/Ca variability in *D. dianthus* may be a coral vital effect responding to changes in the coral environment (such as food supply, microenvironment, or $[CO_3^{2-}]_{seawater}$).

When we remove the high Cd/Ca North Atlantic and Galapagos samples from the calibration and compare to the foraminifera calibration results, we find that the variability in deep-sea corals is comparable to that of the calcitic and aragonitic foraminifera with no evident depth dependence. We believe that Cd/Ca in these samples may reflect the environmental Cd/Ca signal from the seawater with a $D_{Cd/Ca}$ of 1.3 ± 0.1 for *D. dianthus.*

At the moment, our results imply that at least some deep-sea corals are unsuitable for reconstructions of past $[PO_4^{3-}]$. Using Cd/Ca_{coral} as the sole available indicator of coral suitability, we would partition the samples into three groups. Samples like our North Atlantic and Galapagos samples with Cd/Ca_{coral} greater than about 0.20 would be discounted as samples with an obscured environmental signal. Samples with Cd/Ca_{coral} ranging from 0.10 to 0.20 would be interpreted with caution because they could potentially have significant vital effect complications. Samples with Cd/Ca_{coral} between 0 and 0.10 μmol/mol would be interpreted as being a good record of the average nutrient

concentration of the coral growth site. Interpreting the within-coral Cd/Ca record as a record of Cd/Ca_{water} is a separate issue from the accuracy of individual corals. Both modern samples with vertical Cd/Ca transects show an increase in Cd/Ca over the coral lifespan but grew in water with constant Cd/Ca. Therefore, we interpret this increase as a probable vital effect. Corals that show an increase in Cd/Ca over the vertical growth axis (even if Cd/Ca_{coral} is low) may not necessarily be a record of increasing nutrients.

Our fossil samples from 12.0 and 15.4 ka in the North Atlantic and Cd/Ca_{coral} of 0.15–0.70 and 0.10–0.20, respectively. Both records show an increase in Cd/Ca over the coral lifetime (figure 4.11). With a large Cd/Ca_{coral}, we conclude that the record from 12.0 ka does not reflect an environmental signal. The coral from 15.4 ka has a smaller Cd/Ca that falls in the intermediate range described above and possibly reflects Cd/Ca_{water}. The Cd/Ca_{coral} record within the coral does increase over the coral lifetime at a rate between that of the two modern corals. Therefore, the record within this coral may not be a sign of water mass changes in the past.

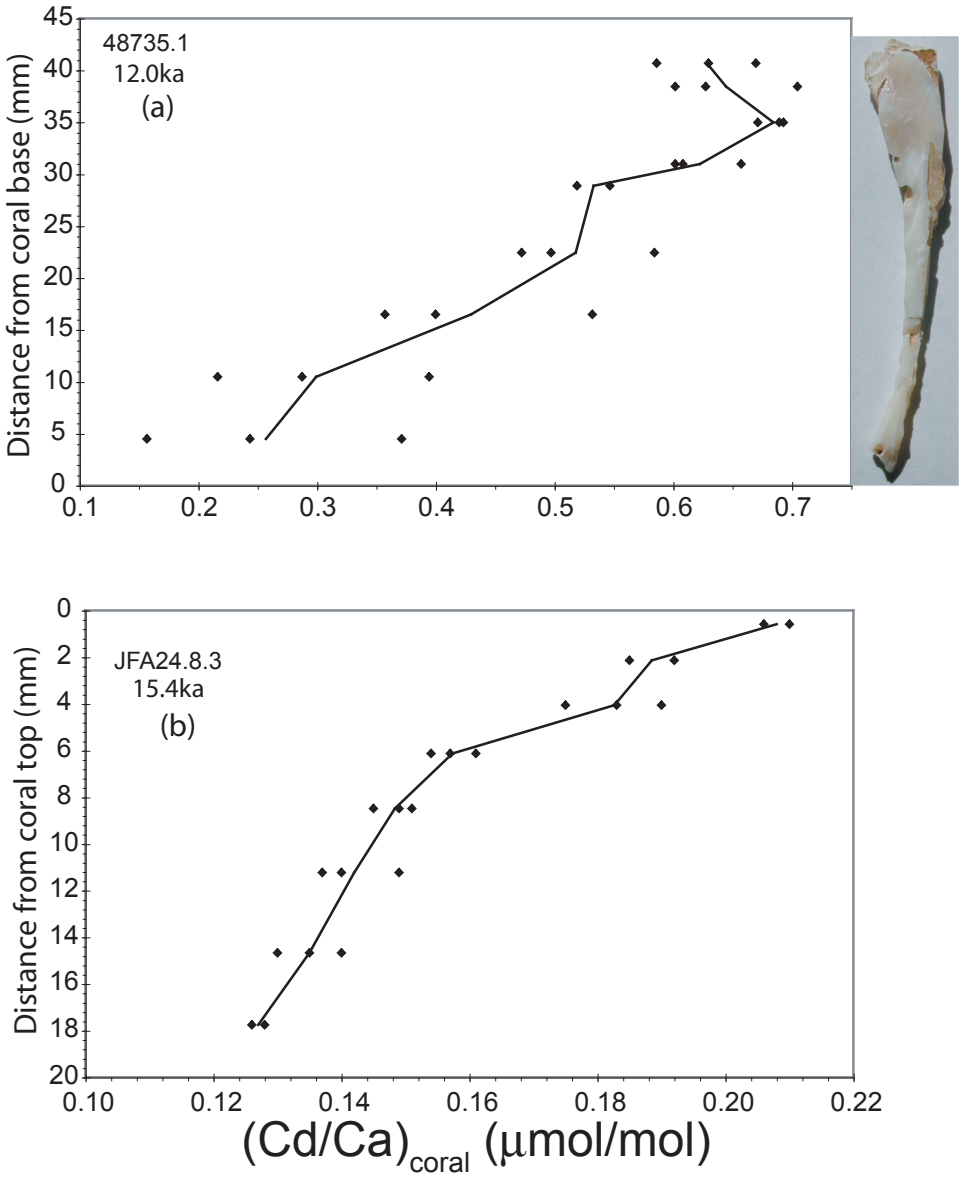

Figure 4.11. Fossil deep-sea coral Cd/Ca results. The upper panel contains the results for the 12.0 ka coral (a) and resembles the results from the high Cd modern corals. Therefore, this coral does not reflect environmental Cd/Ca. The lower panel (b) contains the 15.4 ka fossil coral results from Adkins et al. (1998). This deep-sea coral looks more like the low Cd/Ca corals from the modern calibration, but has a significant increasing trend toward the top of the coral. While this coral probably reflect average ocean Cd/Ca, the increasing trend in the within coral record should be interpreted as an environmental signal with caution because much of the signal could be caused by another mechanism.

Conclusions

Our deep-sea coral Cd/Ca results show that vital effects can obscure the Cd/Ca_{water} signal in deep-sea corals in some cases. We characterize coral vital effects in *D. dianthus* by a high average Cd/Ca_{coral} and large Cd/Ca_{coral} variability within each coral that systematically increases towards the top of the coral. While the systematic trend is present in both high Cd/Ca corals and low Cd/Ca corals, it is most pronounced in the high Cd/Ca corals. When these corals are removed from the calibration data set we see a correlation between Cd/Ca in the coral and Cd/Ca in the seawater that is consistent with a partition coefficient with a value of 1.3 ± 0.1. These results imply that measurements in Cd/Ca in some corals from the past may not be reliable records of seawater Cd/Ca. Therefore, further investigation must be undertaken before Cd/Ca can be considered a reliable proxy for past phosphate concentrations in deep-sea corals.

Bibliography

Adkins, J. F. 1998. Deep-Sea Corals: A New Oceanic Archive, Joint Program in Oceanography/Applied Ocean Science and Engineering, Massachuetts Institure of Technology/Woods Hole Oceanographic Institution, Cambridge.

Adkins, J. F., E. A. Boyle, W. B. Curry, and A. Lutringer. 2003. Stable isotopes in deep-sea corals and a new mechanism for "vital effects." *Geochimica et Cosmochimica Acta* 67 (6):1129-1143.

Adkins, J. F., H. Cheng, E. A. Boyle, E. R. M. Druffel, and R. L. Edwards. 1998. Deep-sea coral evidence for rapid change in ventilation of the deep North Atlantic 15,400 years ago. *Science* 280 (5364):725-728.

Boyle, E. A. 1981. Cadmium, zinc, copper, and barium in foraminifera tests. *Earth and Planetary Science Letters* 53:11-35.

———. 1988. Cadmium: Chemical tracer of deep water paleoceanography. *Paleoceanography* 3:471-489.

———. 1992. Cadmium and d13C paleochemical ocean distributions during the stage 2 glacial maximum. *Annual Review of Earth and Planetary Sciences* 20:245-87.

———. 1995. Limits on benthic foraminiferal chemical analyses as precise measures of environmental properties. *Journal of Foraminiferal Research* 25 (1):4-13.

Boyle, E. A., and L. D. Keigwin. 1985/86. Comparison of Atlantic and Pacific paleochemical records for the last 250,000 years: Changes in deep pcean circulation and chemical inventories. *Earth and Planetary Science Letters* 76:135-150.

Boyle, E. A., L. Lobeyrie, and J.-C. Duplessy. 1995. Calcitic foraminiferal data confirmed by cadmium in aragonitic Hoeglundina: Application to the last glacial maximum in the northern Indian Ocean. *Paleoceanography* 10:881-900.

Boyle, E. A., and Y. Rosenthal. 1996. Chemical hydrography of the South Atlantic during the Last Glacial Maximum: Cd vs d13C. In *The South Atlantic: Past and present circulation*, edited by B. W. Siedler and Webb. Berlin: Springer-Verlag.

Boyle, E. A., F. Sclater, and J. M. Edmond. 1976. On the marine geochemistry of

cadmium. *Nature* 263:42-44.

Delaney, M. L., L. J. Linn, and E. R. M. Druffel. 1993. Seasonal cycles of manganese and cadmium in coral from the Galapogos Islands. *Geochimica et Cosmochimica Acta* 57:347-354.

Elderfield, H., and R. E. M. Rickaby. 2000. Oceanic Cd/P ratio and nutrient utilization in the glacial Southern Ocean. *Nature* 405:305-310.

Frew, R. D., and K. A. Hunter. 1992. Influence of Southern Ocean waters on the cadmium phosphate properties of the global ocean. *Nature* 360:144-146.

Hester, K., and E. A. Boyle. 1982. Water chemistry control of cadmium content in recent benthic foraminifera. *Nature* 298:260-262.

Lea, D. W., and P. A. Martin. 1996. A rapid mass spectrometric method for the simultaneous analysis of barium, cadmium, and strontium in foraminiferal shells. *Geochimica et Cosmochimica Acta* 60 (16):3143-3149.

Linn, L. J., M. L. Delaney, and E. R. M. Druffel. 1990. Trace metals in contemporary and seventeenth-century Galapagos coral: Records of seasonal and annual variations. *Geochimica et Cosmochimica Acta* 54:387-394.

McCorkle, D. C., P. A. Martin, D. W. Lea, and G. P. Klinkhammer. 1995. Evidence for a dissolution effect on benthic foraminiferal shell chemistry: d13C, Cd/Ca, Ba/Ca, and Sr/Ca results from the Ontong Java Plateau. *Paleoceanography* 10 (4):699-714.

Reuer, M. K., E. A. Boyle, and J. E. Cole. 2003. A mid-twentieth century reduction in tropical upwelling inferred from coralline trace element proxies. *Earth and Planetary Science Letters* 210:437-452.

Rickaby, R. E. M., M. J. Greaves, and H. Elderfield. 2000. Cd in planktonic and benthic foraminiferal shells determined by thermal ionisation mass spectrometry. *Geochimica et Cosmochimica Acta* 64 (7):1229-1236.

Rosenthal, Y., P. M. Field, and R. M. Sherrell. 1999. Precise determination of element/calcium ratios in calcareous samples using sector field inductively coupled plasma mass spectrometry. *Analytical Chemistry* 71 (15):3248-3253.

Shen, G. T., and E. A. Boyle. 1988. Determination of lead, cadmium and other trace metals in anually-banded corals. *Chemical Geology* 67:47-62.

Shen, G. T., E. A. Boyle, and D. W. Lea. 1987. Cadmium in corals as a tracer of

historical upwelling and industrial fallout. *Nature* 328:794-796.